

Photophysical properties of multiply phenylated C_{70} derivatives: Spectroscopic and quantum-chemical investigations

P.-F. Coheur^{a)}

Laboratoire de Chimie Physique Moléculaire, Université Libre de Bruxelles, CP 160/09, 50 av. F. D. Roosevelt, B-1050 Brussels, Belgium

J. Cornil^{a)} and D. A. dos Santos

Service de Chimie des Matériaux Nouveaux, Centre de Recherche en Electronique et Photonique Moléculaires, Université de Mons-Hainaut, Place du Parc 20, B-7000 Mons, Belgium

P. R. Birkett

Fullerene Science Centre, CPES School, University of Sussex Brighton, BN1 9QJ, United Kingdom

J. Liévin

Laboratoire de Chimie Physique Moléculaire, Université Libre de Bruxelles, CP 160/09, 50 av. F. D. Roosevelt, B-1050 Brussels, Belgium

J. L. Brédas

Service de Chimie des Matériaux Nouveaux, Centre de Recherche en Electronique et Photonique Moléculaires, Université de Mons-Hainaut, Place du Parc 20, B-7000 Mons, Belgium and Department of Chemistry, The University of Arizona, Tucson, Arizona 85721-0041

D. R. M. Walton, R. Taylor, and H. W. Kroto

Fullerene Science Centre, CPES School, University of Sussex Brighton, BN1 9QJ, United Kingdom

R. Colin^{b)}

Laboratoire de Chimie Physique Moléculaire, Université Libre de Bruxelles, CP 160/09, 50 av. F. D. Roosevelt, B-1050 Brussels, Belgium

(Received 22 September 1999; accepted 4 January 2000)

The photophysics of six multiply phenylated C_{70} derivatives [$C_{70}Ph_2$, $C_{70}Ph_4$, $C_{70}Ph_6$ (two regioisomers), $C_{70}Ph_8$ and $C_{70}Ph_{10}$] have been investigated by means of steady state spectroscopy in cyclohexane solution and quantum-chemical calculations derived from semiempirical Hartree–Fock approaches. There is good agreement between the measured absorption spectra and the INDO/SCI calculated excitation energies for each derivative. The foregoing results and some additional ground state properties calculated at the AM1 level have been used to predict that the perturbation of the π electronic system of the cage results in significant changes in the photophysics of the fullerene derivatives. The effects of conjugation and spatial localization of the HOMO and LUMO orbitals on the energy of the first electronic transition are discussed in greater detail. © 2000 American Institute of Physics. [S0021-9606(00)00113-6]

INTRODUCTION

Fullerenes C_{60} and C_{70} possess many interesting properties including remarkable nonlinear optical behavior and ability to sensitize oxygen upon photoexcitation. These properties, which rely on the photophysical characteristics of the molecules,¹ have produced opportunities for their use as optical limiters² or photodynamic agents.^{3,4} The discovery that C_{60} and C_{70} are chemically reactive has considerably widened the field of potential applications to include new classes of functionalized molecules, all of which have specific properties that require characterization. Indeed, as the functionalization of the fullerenes requires addition to C–C double bonds, it is expected that the resulting derivatives have photophysical properties different from those of the parent molecule. Extensive studies of monofunctionalized C_{60} deriva-

tives have, however, shown these molecules to retain most of the spectral signatures of C_{60} .^{1,5–17} In contrast, very few studies examined the photophysical behavior of multifunctionalized fullerene derivatives^{7,8,18–24} (especially derivatives of C_{70} and higher fullerenes). Such multifunctionalization initiates a larger perturbation of the cage π electronic system and, as a result, the molecules may exhibit more unusual optical properties compared to those of the parent and monofunctionalized fullerenes. In another paper, we described the spectroscopic properties of five hexafunctionalized C_{60} derivatives, which differ only in their functional groups or their geometrical configurations.²⁵ As a result of the geometric and electronic changes to the fullerene cage in the foregoing molecules, significant modifications of both the ground and excited states with respect to C_{60} were observed. These results, however, lead us to conclude that the nature of the addends/substituents has, in these examples, little effect on the spectroscopic properties of the molecules, even though there are significant changes to their one-electron properties

^{a)}P.-F.C. is FRIA grant holder and J.C. is a FNRS research fellow.

^{b)}Electronic mail: rcolin@ulb.ac.be

(especially the ionization potential and the electron affinity). This paper analyzes multiply phenylated derivatives of C_{70} [$C_{70}Ph_2$, $C_{70}Ph_4$, $C_{70}Ph_6$ (two regioisomers are considered for the calculations), $C_{70}Ph_8$ and $C_{70}Ph_{10}$] in order to extend the former study. As each of the $C_{70}Ph_{2n}$ ($n=1$ to 5) derivative results in specific changes to the π electronic system of the cage, we are able to examine how the modified π system reflects upon the photophysical properties of these molecules. Furthermore, the determination of the photophysical properties of these $C_{70}Ph_{2n}$ derivatives is of particular interest as two of them ($n=4$ and 5) exhibit strong eye-detectable luminescence.²⁶ This type of behavior is, to date, unusual in fullerene chemistry; to the best of our knowledge there are only two other well-characterized fullerene derivatives, T_h and D_3 regioisomers of a hexapyrrolidine derivative of C_{60} ,²³ which display similar photophysical properties. Interestingly, the luminescence of the hexapyrrolidino- C_{60} derivative (in a polymer blend) proved to be adequate for the fabrication of an organic white light emitting diode (LED).²⁴ In the present study of $C_{70}Ph_{2n}$ derivatives, we have taken the same experimental and theoretical approach as in our analysis of C_{60} derivatives.²⁵

EXPERIMENTAL AND THEORETICAL METHODS

Synthesis

The detailed syntheses and characterization of the $C_{70}Ph_8$ and $C_{70}Ph_{10}$ samples have been published previously;²⁶ similar data on the other $C_{70}Ph_{2n}$ derivatives will be the object of a forthcoming paper.²⁷

Spectroscopic measurements

A small quantity of each material was dissolved in cyclohexane (spectroscopic grade); concentrated ($\sim 10^{-5}$ mol l⁻¹) and dilute solutions ($\sim 10^{-6}$ mol l⁻¹) were prepared. Due to the small amount of material available, the concentration of these solutions were not more precisely determined. Absorption spectra were recorded with a HP 8452A spectrophotometer in the 210–820 nm spectral range by increments of 2 nm. The concentrated and dilute solutions of each derivative were used to record their absorption spectra in the visible and the UV region, respectively. Fluorescence spectra of each of the more concentrated solutions were recorded with a Shimadzu RF-5001PC spectrofluorometer.

Quantum-chemical calculations

The structure of each derivative was deduced using NMR spectroscopy. The structures presented for $C_{70}Ph_2$ and $C_{70}Ph_4$ are the predicted, preferred isomers (of a total of four and three, respectively) which satisfy the experimental data²⁷ while both of the possible regioisomers of $C_{70}Ph_6$ which fit the NMR data²⁷ are considered. Using these structures, the nuclear coordinates of each derivative were generated at the molecular mechanics level using the universal force field

method.²⁸ Adopting the latter coordinates as a starting point, the geometries of the derivatives were further optimized at the semiempirical Hartree–Fock Austin Model 1 (AM1) level,²⁹ as implemented in the GAUSSIAN 94 package.³⁰

As in our study of the hexa-functionalized C_{60} derivatives,²⁵ the AM1 calculated ground-state properties we pay most attention to in this paper are the heat of formation, the atomic charge distribution as obtained by a Mulliken population analysis,³¹ the ionization potential (I) and electron affinity (A) approximated by Koopmans theorem.³² The graphical representations of the HOMO and LUMO orbitals (graphical interface Insight II of Molecular Simulations Inc.³³) and their spatial localization, expressed in term of the participation number PN,³⁴ are obtained on the basis of the LCAO coefficients calculated at the INDO/S level. Within this formalism, the PN writes (e.g., Refs. 25 and 35):

$$PN = \frac{[\sum_{\lambda} c_{i\lambda}^2]^2}{\sum_{\lambda} c_{i\lambda}^4}, \quad (1)$$

where $c_{i\lambda}$ is the LCAO coefficient on the λ th atom in the i th molecular orbital.

The fundamental electronic configurations of the phenylated C_{70} derivatives are all closed-shell systems, defining an electronic ground state of singlet multiplicity S_0 . In the following, we only consider the electric dipole allowed transitions from S_0 to the manifold of electronic excited singlet states S_n , which are expected to dominate the absorption spectrum in the UV and the visible. The calculations of the vertical S_0 – S_n excitation energies and oscillator strengths are performed using the semiempirical Hartree–Fock INDO/S method³⁶ and a single configuration interaction (SCI) technique. The Mataga–Nishimoto potential³⁷ is used to express the electron interaction terms. The early INDO/SCI calculations of Bendale *et al.*³⁸ on C_{60} and C_{70} have shown the adequacy of this theoretical approach for the modeling of the absorption spectra of fullerenes in the visible and UV regions up to 5 eV. Above this energy limit, the calculated oscillator strengths were markedly underestimated with respect to the experimental data. Similarly an upper limit is to be expected for the present INDO/SCI calculations³⁹ and we have therefore chosen to consider only the electronic transitions with energies lower than 5 eV. By analogy with our study on the C_{60} derivatives,²⁵ we have included a maximum of 5625 excited configurations in the calculations (this number corresponds to all single excitations from the 75 highest occupied to the 75 lowest unoccupied MOs). The resulting data, which constitute a “bar spectrum” (vertical excitation energies vs oscillator strengths) are used to analyze the absorption spectra in the present work. To more adequately model the observed spectra over the entire spectral range, we also use a “synthetic spectrum,” obtained by convoluting the “bar spectrum” with a Gaussian function of given full width at half-maximum (FWHM).

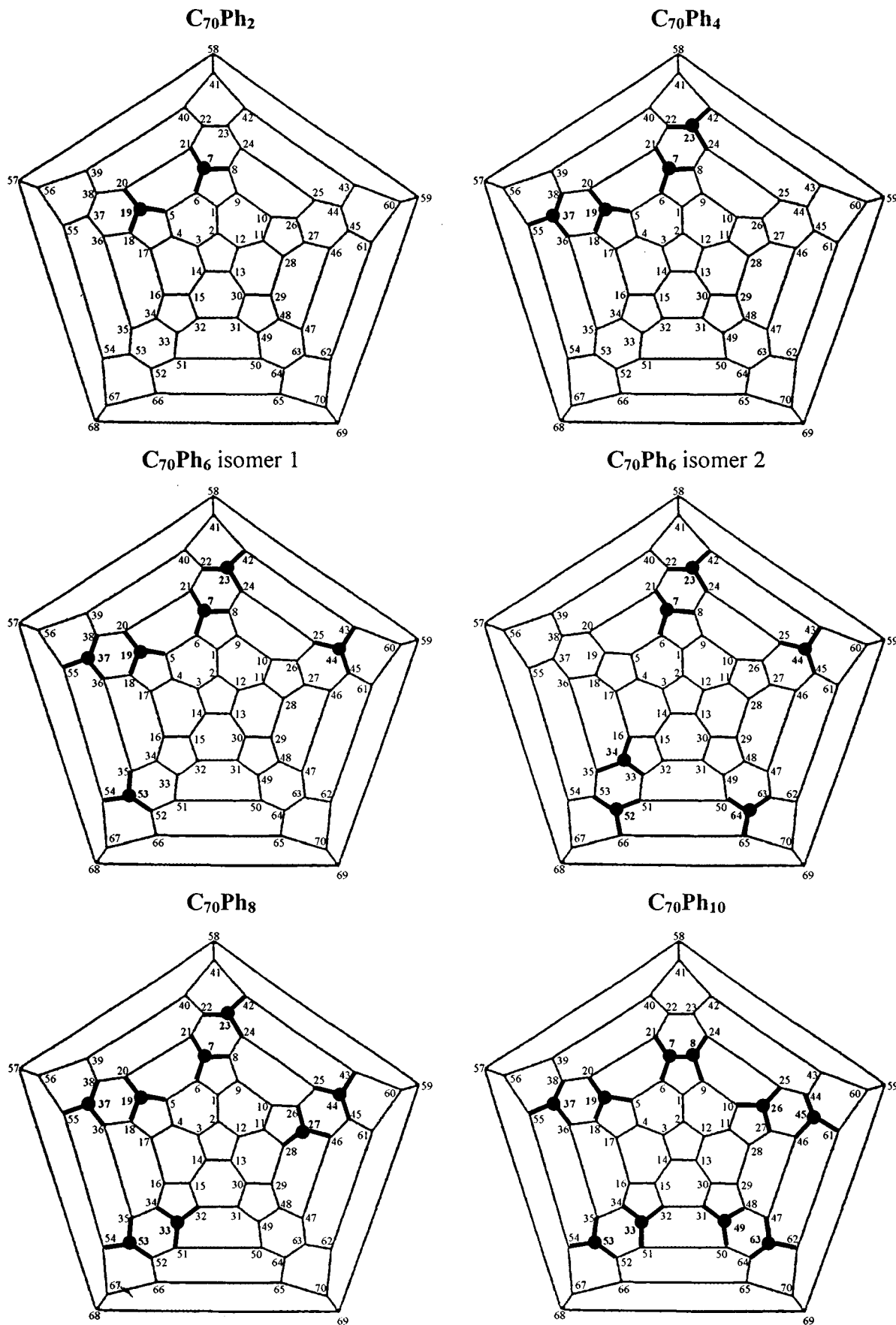


FIG. 1. Schlegel diagrams giving the geometric configuration of the $C_{70}Ph_{2n}$ derivatives ($n=1$ to 5). The black balls represent the phenyl groups and the heavy black line represents the single $C-C$ bonds involving a sp^3 carbon atom of the C_{70} cage.

RESULTS

Geometry

The geometric configuration of the phenylated derivatives is visualized with the help of Schlegel diagrams in Fig. 1. The numbering of the cage carbon atoms is that adopted by IUPAC.⁴⁰ Each molecule is at first glance characterized by a plane of symmetry; however, the phenyl groups are in fact not oriented symmetrically with respect to one another in their lowest energy conformations. The configuration of the molecules under study is therefore rather that of a *pseudo-C_s*-symmetrical type.²⁵ In the case of C₇₀Ph₆, it should be noted that although both regioisomers depicted in Fig. 1 fit the NMR data, and that isomer 2 is the preferred thermodynamic product, the structure shown as isomer 1 is considered to be the most likely for the derivative due to the favorable addition mechanism underlying its formation.²⁷

As a result of the weaker strain required for closure of the carbon cage of C₇₀ compared with that of C₆₀, it is well known that the delocalized character of the electronic system is higher in the former molecule. This is confirmed, for example, by the existence of bonds of intermediate length on the C₇₀ cage. By analogy to the AM1 calculated bond lengths (**d**) for C₇₀, we consider for the phenylated derivatives under study: (i) *single bonds* (with **d** > 1.434 Å); (ii) *intermediate bonds* (for which 1.387 ≤ **d** ≤ 1.434 Å); and (iii) *double bonds* (with **d** < 1.387 Å). A simple method of specifying the distinctive bonding for each multiply phenylated derivative consists then in listing and counting the bonds that belong to the above-defined groups (see Table I). In Table I, the single C–C bonds have been further subdivided into two classes: those single bonds which result from the presence of *sp*³ carbon atoms (for which **d** > 1.500 Å) and those implying the presence of *sp*² carbon atoms, respectively. It is observed, from the data presented in Table I, that the number of bonds involving *sp*³ carbon atoms increases linearly with the number of attached groups. In contrast, no such regularity can be distinguished within the other classes of bonds as one moves from one derivative to the next. This is especially true for the number of bonds which are of intermediate length and which can be considered, to a first approximation, as a measure of the degree of conjugation of the electronic system on the cage. From Table I, therefore, it can be noted that the predicted C₇₀Ph₆ isomer (isomer 1) and C₇₀Ph₁₀ are, respectively, the most and the least conjugated derivative. All of the other derivatives analyzed fall between these two extreme cases, including C₇₀, which we have used as a reference. It should be noted that electronic conjugation over the entire cage is necessarily limited for C₇₀Ph₁₀ because of the presence of the *sp*³ carbon atoms that isolate two π electronic systems from one another (see Fig. 1).

Ground-state properties

The heats of formation calculated at the AM1 level are given in Table II. As the molecules have similar chemical composition the calculated values should, in principle, be consistent throughout the C₇₀Ph_{2*n*} series and should therefore allow a stability sequence to be established. The results reveal that the heat of formation increases with the number of

phenyl groups attached to the C₇₀ cage with a steplike evolution. C₇₀Ph₂ and C₇₀Ph₄ are characterized by a similar ΔH_f value of 1111 ± 1 kcal mol⁻¹, which is larger than that of C₇₀ (1061 kcal mol⁻¹) but smaller than that of C₇₀Ph₆ isomer 1 and C₇₀Ph₈ (1154 ± 2 kcal mol⁻¹). The latter value is in turn smaller than that of C₇₀Ph₁₀ (1185 kcal mol⁻¹). Only isomer 2 of C₇₀Ph₆ lies slightly off sequence; its calculated heat of formation (1145 kcal mol⁻¹) confirms that it is more stable than the predicted structure of isomer 1.

The net atomic charges reported in Table II, which are obtained by a Mulliken population analysis within the AM1 formalism, are summed over the phenyl groups (the average value per phenyl is given for each derivative) and the C₇₀ cage. The phenyl groups are in all of the investigated cases electron-donating with respect to the cage, as was also reported for phenylated C₆₀ derivatives.²⁵ Furthermore, the calculations indicate that the electron-donating character per phenyl group diminishes as the number of such groups attached to the fullerene cage increases. For example, the mean value per phenyl group is calculated to be +0.044 |*e*| in C₇₀Ph₂ and +0.029 |*e*| in C₇₀Ph₁₀. The total charge donated to the cage is however a maximum for C₇₀Ph₁₀ (+0.292 |*e*|) and, interestingly, one can show that the charge excess is redistributed similarly over the two independent π electronic subgroups defined above in this derivative.

The graphical representation of the HOMO and LUMO and their corresponding PN are given in Fig. 2. From Fig. 2 it can be seen that HOMOs and LUMOs differ strongly within the series of derivatives. For example, the HOMOs of C₇₀Ph₈ and the C₇₀Ph₆ isomers are localized on the cage (with a PN of about 31) whereas those of C₇₀Ph₂, C₇₀Ph₄, and C₇₀Ph₁₀ are more strongly delocalized (PN of 47.3, 48.7, and 50.9, respectively) and do not necessarily involve the same carbon atoms. The same results are observed for the LUMOs. For both HOMOs and LUMOs, we note that the phenyl groups make little contribution.

The AM1 and INDO ionization potentials (*I*) and electron affinities (*A*) calculated within Koopman's theorem are given in Table II. The AM1 HOMO and LUMO energy levels ($E_{\text{HOMO}} = -I$ and $E_{\text{LUMO}} = -A$) are further represented on a scaled diagram (Fig. 3) in order to display the HOMO–LUMO energy difference ($\Delta E = I - A$) and the deviations with respect to the energy levels calculated for C₇₀. The AM1 results show that with the exception of the LUMO of C₇₀Ph₂, all other molecular orbitals are somewhat destabilized with respect to those in C₇₀. The HOMO and LUMO are, however, not destabilized by a similar amount as one moves down the series of C₇₀Ph_{2*n*} (increasing *n*) and, as a consequence, ΔE has values ranging from 4.90 eV for C₇₀Ph₆ isomer 1 to 7.07 eV for C₇₀Ph₁₀. The INDO/S data yield a similar pattern although notable differences are obvious in the absolute orbital energy values as in the destabilization energies calculated with respect to C₇₀ (see Table II).

Spectroscopic properties

The absorption and fluorescence spectra of each derivative dissolved in cyclohexane are given in Fig. 4; the corresponding spectra recorded for C₇₀ are shown for the sake of

TABLE I. Counting of the bonds on the C₇₀ cage according to their single, intermediate or double character (see text for details).

	C ₇₀	C ₇₀ Ph ₂	C ₇₀ Ph ₄	C ₇₀ Ph ₆			
				Isomer 1	Isomer 2	C ₇₀ Ph ₈	C ₇₀ Ph ₁₀
Single bonds (C- <i>sp</i> ³ C)	0	6	12	18	18	24	30
Single bonds (C- <i>sp</i> ² C)	64	60	52	41	48	43	38
Double bonds	20	15	16	14	15	18	18
Intermediate bonds	21	24	25	32	24	20	19

comparison. In Fig. 4, optical densities (OD) are used to characterize the absorption (extinction coefficients could not be determined due to the very small quantity of material available); the fluorescence spectra are in arbitrary units. The main photophysical quantities measured from these spectra are reported in Table III.

The results show that the derivatives have similar absorption spectra in the UV, dominated by bands at 230 ± 8 nm and 296 ± 4 nm; we note that the former band is reminiscent of the absorption of C₇₀ and that the second band is not clearly detectable for C₇₀Ph₁₀. Compared to the parent C₇₀ molecule, the absorption spectra of the derivatives appear less resolved. This is expected from the lowering of the symmetry induced by the functionalization of the fullerene cage. In addition, we note that contrarily to the other three derivatives, C₇₀Ph₈ and C₇₀Ph₁₀ have their absorption spectra blueshifted with respect to C₇₀. One important point for the following discussion comes from the fact that the spectra of the derivatives in the visible region are very different from one another. This can, for example, be seen clearly by observing the position of the lowest-energy absorption band, which lies in the two extreme cases at 780 nm (C₇₀Ph₂) and 472 nm (C₇₀Ph₁₀).

For each derivative, the fluorescence band lies close to the longest wavelength band of the absorption spectrum (Fig. 4). Since fluorescence remains unchanged when modifying the excitation wavelength, we can conjecture that these two bands are due to the S₁ ← S₀ (absorption) and S₁ → S₀ (fluorescence) transitions. An experimental determination of the S₁ energy with respect to S₀ is therefore provided by averaging the energy measured at the maximum of the two corresponding bands; these values of S₁ are reported in Table III. One should note that for some derivatives the fluores-

cence spectrum reveals more than a single band. The bands lying to the red side of the fluorescence maximum are likely to be vibrational components of the S₁ – S₀ electronic transition and are accordingly also reported in Table III. On the other hand, we have disregarded the very weak features that are observed in some cases to the blue side of the fluorescence maximum as these bands originate probably from traces of other C₇₀Ph_{2*n*} molecules in the sample. We note finally that the fluorescence spectra recorded for C₇₀Ph₈ and C₇₀Ph₁₀ in cyclohexane at room temperature are in good agreement with the fluorescence measurements made by Groenen *et al.* for the molecules in decalin/cyclohexane at 4.2 K.⁴¹

For C₇₀Ph₂, C₇₀Ph₄, C₇₀Ph₈, and C₇₀Ph₁₀, the INDO/SCI calculations (including 5626 configurations) produce a good agreement with the measured absorption spectra over the entire spectral range (even though the convergence of the high lying S_n – S₀ excitation energies and oscillator strengths is as expected not fully reached for the largest molecules). The high quality of the agreement between the measured and calculated data in the visible region allows the assignment of the spectral features to specific electronic transitions. In particular we show that, for these derivatives, the lowest lying absorption band and the fluorescence band correspond to the first electronic transition S₁ – S₀ (see Table III).

The comparison between the measured and calculated values of the S₁ – S₀ transition suggest that isomer 2 of C₇₀Ph₆ is responsible for the fluorescence at 728 nm and the lowest absorption band. We note, however, that isomer 2 is not the predicted C₇₀Ph₆ isomer and moreover that it does not account for all the absorption bands characteristic of C₇₀Ph₆ in the visible region [Fig. 5(a)]. A reasonable agree-

TABLE II. Ground-state properties (heat of formation Δ*H*_f, charge distribution, ionization potential *I*, electron affinity *A*, and HOMO–LUMO gap Δ*E*) calculated at the AM1 level. The total charge transferred towards the cage and the average contribution of the phenyl groups are given. The INDO/S values for *I*, *A*, and Δ*E* are given in parentheses.

	C ₇₀	C ₇₀ Ph ₂	C ₇₀ Ph ₄	C ₇₀ Ph ₆			
				Isomer 1	Isomer 2	C ₇₀ Ph ₈	C ₇₀ Ph ₁₀
Δ <i>H</i> _f (kcal mol ⁻¹)	1061	1111	1112	1152	1145	1156	1185
Charge distribution (<i>e</i>)							
on C ₇₀ cage		-0.088	-0.161	-0.219	-0.228	-0.265	-0.292
per phenyl on average		+0.044	+0.040	+0.037	+0.038	+0.033	+0.029
<i>I</i> (eV)	9.14(6.51)	8.45(5.91)	8.80(6.36)	8.11(5.72)	8.51(6.16)	8.74(6.47)	8.83(6.44)
<i>A</i> (eV)	3.27(1.18)	3.35(1.45)	2.88(1.12)	3.21(1.72)	2.65(1.23)	2.23(0.86)	1.76(0.60)
Δ <i>E</i> (eV)	5.87(5.33)	5.10(4.46)	5.92(5.24)	4.90(4.00)	5.86(4.93)	6.51(5.61)	7.07(5.84)

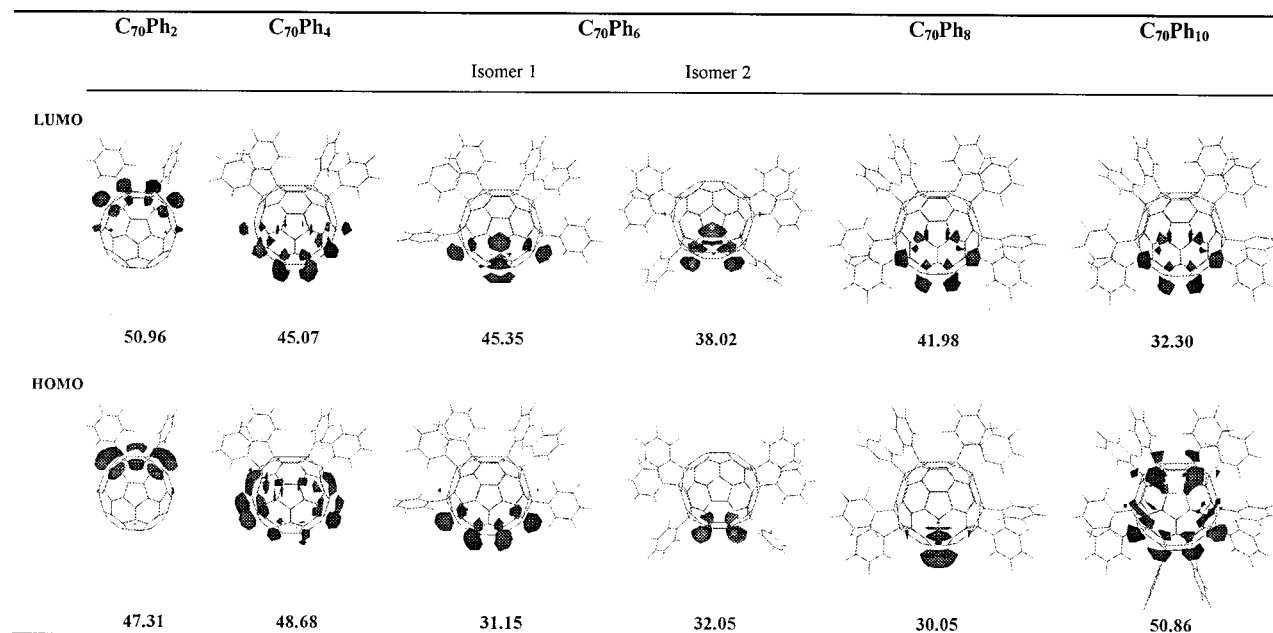


FIG. 2. Graphical representation of the HOMO and LUMO orbitals on the basis of the INDO/S optimized LCAO coefficients. The participation number PN is given below each orbital representation.

ment between the calculated spectrum of isomer 1 with the experimental data is only obtained when a rigid redshift of about 2000 cm^{-1} for all transitions is adopted. This implies that fluorescence is due to the radiative relaxation from the S_2 state and that a low-lying band exists at 1400 nm [Fig. 5(b)]; preliminary experiments in the near-IR region (by using a Perkin-Elmer spectrophotometer sensitive up to 1100 nm), have failed to prove this hypothesis. Finally, we note that the best agreement between calculated and experimental

data is obtained when considering a 50–50 contribution of both isomers to the absorption spectrum [see Fig. 5(c)]; the fluorescence would in that case be that due to isomer 2. The $C_{70}Ph_6$ sample studied is very unlikely, however, to have more than one regioisomer present in view of its characteristic NMR spectra.²⁷ It is evident from the above observations that a definitive assignment for the spectral features of $C_{70}Ph_6$ should therefore await new experimental and theoretical investigations.

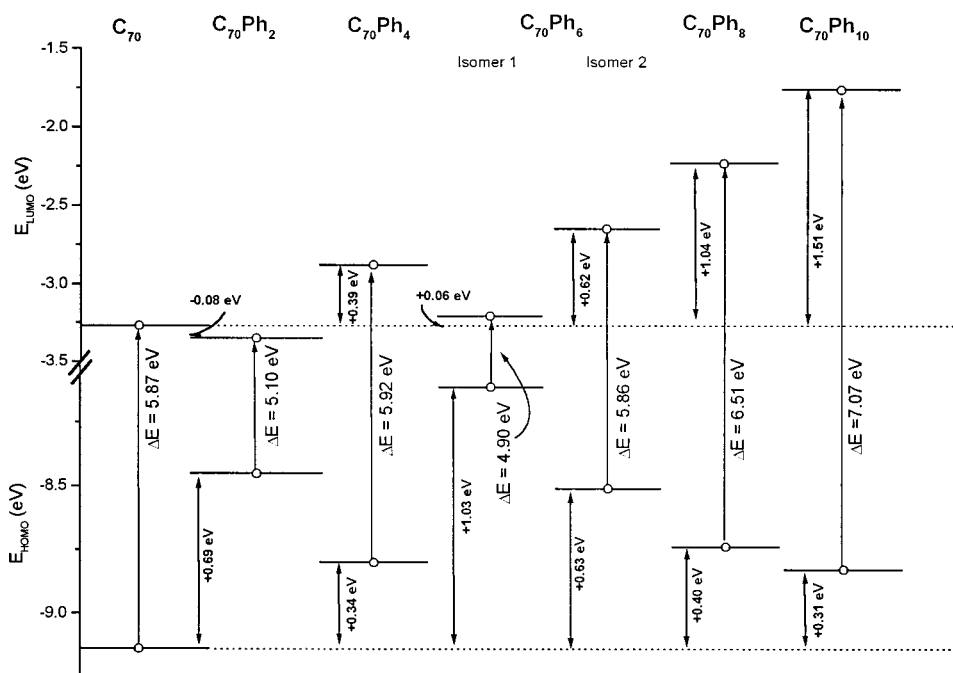


FIG. 3. AM1 energies for the HOMO and LUMO orbitals. The dashed lines represent the energy reference for the orbitals of C_{70} , from which destabilization effects are measured (double arrows). The calculated value of the HOMO–LUMO gap ΔE is also shown.

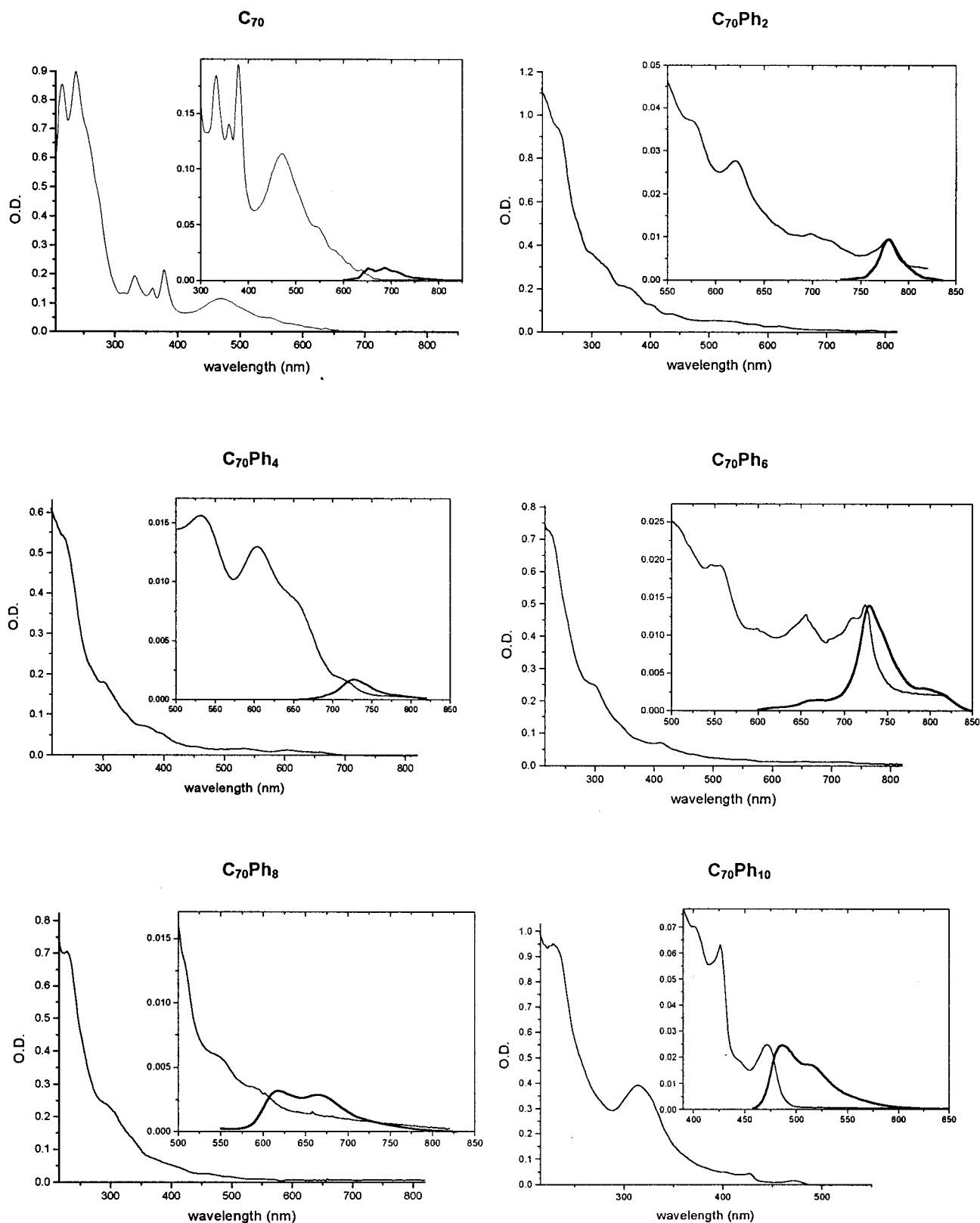


FIG. 4. UV-visible absorption (thin line) and fluorescence (thick line) spectra for C_{70} and the $C_{70}Ph_{2n}$ derivatives dissolved in cyclohexane. The intensity of the fluorescence spectra are expressed in arbitrary units.

DISCUSSION

The foregoing bond-length analysis and calculated one-electron properties (ionization potential, electron affinity, spatial localization of HOMO and LUMO) have shown that

the geometry and electronic structure are specific for each $C_{70}Ph_{2n}$ derivative studied and that these properties are also very different from those of the parent C_{70} molecule. As expected, the strong perturbation induced by the multifunc-

TABLE III. Main photophysical properties measured from the absorption and fluorescence spectra. The INDO/SCI value for the vertical excitation energy S_1-S_0 is also given.

	C ₇₀ Ph ₂	C ₇₀ Ph ₄	C ₇₀ Ph ₆	C ₇₀ Ph ₈	C ₇₀ Ph ₁₀	C ₇₀
Absorption bands (λ, nm)	238	232	222	229	228	238
						252
	294	300	296	292		
					314	314
						332
	352			364	380	{360
						{378
	402	396	411	396	402	
	436		438		426	
					443	
		452	466	458	472	470
	505		505	{495		
				{502		
	540	{532	546	545		542
		{545				
576		556				
620	606	598	590		{592	
					{612	
					{638	
	645	655				
696	682	708				
720	714	724				
780						
Fluorescence band (λ, nm)						
Maximum	780	721	728	617	487	652
Additional features		783	738	664	511	
			795			
			815			
S₀-S₁ excitation energy (eV)						
Measured	1.59	1.73	1.72	2.03	2.58	1.92
Calculated	1.51	2.14	{1.12 (isomer 1)	2.38	2.67	2.15
			{1.88 (isomer 2)			

tionalization of the cage has important effects on the photophysical properties of these molecules. This is essentially revealed by the distinctive absorption system each derivative displays in the visible region, as well as by their fluorescence spectra. In this discussion, we will focus on the first electronic transition S_1-S_0 .

We have, in first instance, investigated the effect of the cage conjugation on the energy of the lowest electronic transition. The results are given in Fig. 6, where the calculated vertical excitation energies S_1-S_0 for C₇₀ and each derivative are plotted versus the degree of conjugation on the cage (estimated in a simplified manner from the number of bonds being of intermediate length between single and double bonds). The two quantities correlate well, suggesting, as expected, that the stronger the conjugation on the cage the smaller the S_1-S_0 energy separation. For example, C₇₀Ph₆ isomer 1 and C₇₀Ph₁₀, which are the most and the least conjugated derivatives, have the lowest and highest S_1-S_0 vertical excitation energies of 1.12 eV and 2.67 eV, respectively. The deviation from a linear relationship that normally applies for conjugated systems⁴² is not surprising if one considers the degree of simplicity of the model. Interestingly, Fig. 6 shows that the different spectroscopic properties of the C₇₀Ph₆ isomers (which coincide reasonably well with the se-

quence) can be partly rationalized in terms of conjugation effects.

The spatial localization of HOMO and LUMO levels, which is known to influence the energy of these orbitals and consequently the value of the HOMO-LUMO gap ΔE (see for instance Ref. 35), offers an alternative explanation for the different S_1-S_0 energies reported. The correlation between the spatial localization (expressed in term of the participation number PN) and energy of the HOMO and LUMO levels calculated either at the AM1 or INDO/S level is poorer than expected (see Fig. 7). The only distinguishable trend that can be observed from these data is that the energy of the LUMO level appears to decrease as delocalization on the cage increases (larger value of PN).

It is interesting to compare the photophysical properties of the C₇₀Ph_{2n} derivatives investigated, to the results obtained by Schick *et al.*^{23,24} for the photophysics of two regioisomers (T_h and D_3 symmetric) hexapyrrolidino-derivative of C₆₀. These C₆₀ derivatives are strongly luminescent, as are the C₇₀Ph_{2n} derivatives studied in this work (especially C₇₀Ph₈ and C₇₀Ph₁₀ which show strong eye-detectable luminescence²⁶). Schick *et al.* have explained the peculiar photophysical behavior of hexapyrrolidine fullerene derivatives by suggesting that a diminished π system on the

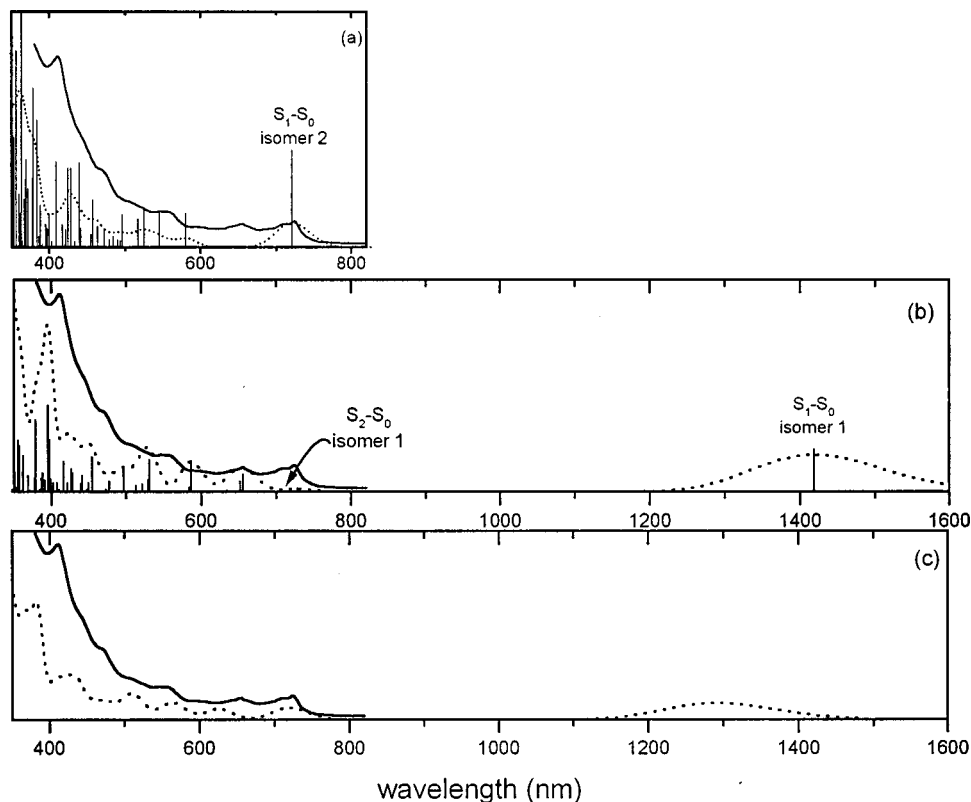


FIG. 5. Absorption (solid line) and INDO/SCI "bar" and "synthetic" (dotted line) spectra of $C_{70}Ph_6$ in the visible region (Gaussian functions having a FWHM of 1000 cm^{-1} are used to generate the "synthetic" spectra). In (a) the calculated spectra correspond to isomer 2 and are rigidly redshifted by 1300 cm^{-1} while in (b) they correspond to isomer 1 and are rigidly redshifted by 2000 cm^{-1} . In (c) the calculated "synthetic" spectrum represents the 50–50 contribution of isomer 1 and isomer 2, rigidly redshifted, as in (a), by 1300 cm^{-1} so as to have correspondence between the calculated vertical S_1-S_0 energy for isomer 2 and the absorption band measured at 724 nm .

cage induces a greater energy separation between the S_0 ground state and both the first excited singlet and triplet states (S_1 and T_1). Thus the radiative rate from S_1 increases while the rate of radiationless transition from T_1 decreases. Our results fully corroborate these conclusions about the relationship between the S_1-S_0 gap and the degree of conjugation on the cage (Fig. 6). Furthermore, preliminary attempts to characterize the relative fluorescence intensity of the $C_{70}Ph_{2n}$ derivatives with respect to one another also tend to confirm, as suggested by Schick *et al.*, that the fluorescence increases as the cage π system diminishes or accordingly, as the S_1-S_0 energy separation increases. In particular, the strongly luminescent $C_{70}Ph_{10}$ and $C_{70}Ph_8$ derivatives

are the least conjugated $C_{70}Ph_{2n}$ derivatives investigated and are characterized by a high-energy first electronic transition. To assess the validity of the present results, the fluorescence quantum yield of each of the $C_{70}Ph_{2n}$ derivative should, however, be precisely determined.

CONCLUSIONS

We have described the photophysical properties of six multifunctionalized derivatives of C_{70} : $C_{70}Ph_2$, $C_{70}Ph_4$, $C_{70}Ph_6$ (two isomers are considered for the theoretical work), $C_{70}Ph_8$, and $C_{70}Ph_{10}$. The analysis of the absorption and fluorescence spectra of each derivative was based on INDO/

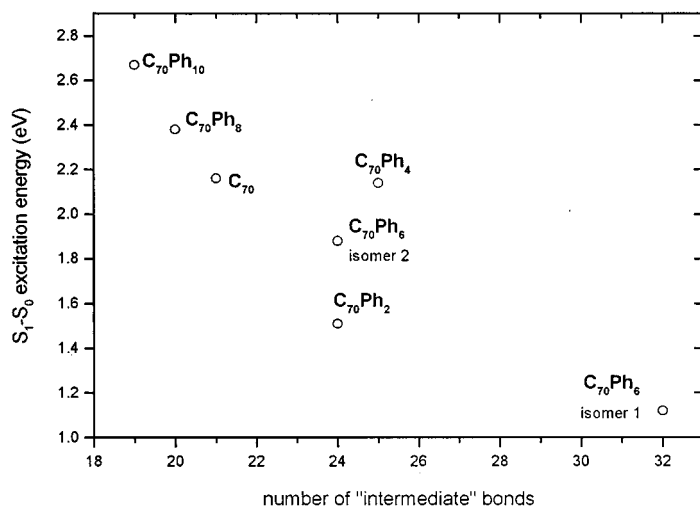


FIG. 6. Correlation between the conjugation on the C_{70} cage, expressed in term of the "number of bonds with intermediate length," and the vertical S_1-S_0 excitation energy (eV).

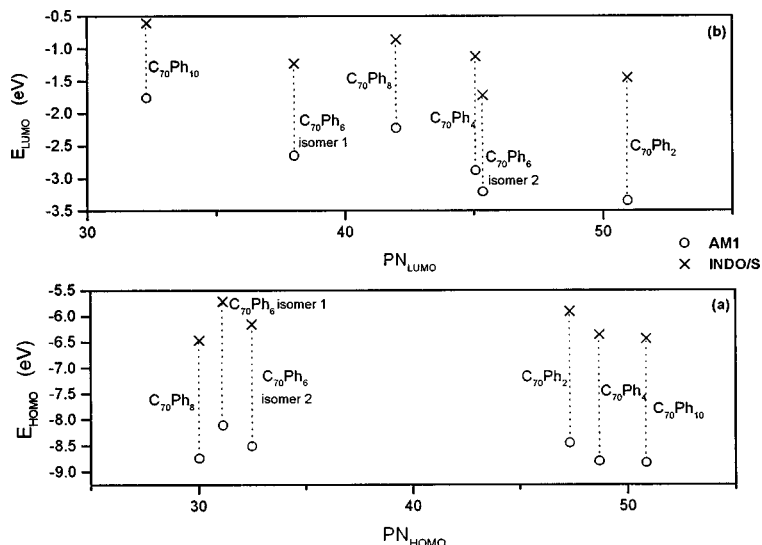


FIG. 7. Correlation between the spatial localization of the HOMO and LUMO orbitals on the cage, expressed in terms of the participation number PN, and their respective energies. The circles and the crosses give the AM1 and INDO/S calculated energy values, respectively.

SCI calculations involving 5625 excited configurations. Particular attention was paid to the first electronic transition and to the changes observed in it due to the degree of perturbation of the cage π electronic system. We have shown that the cage conjugation simply expressed in terms of geometric arguments plays an important part in influencing the photophysical properties of fullerene derivatives: weaker conjugation induces a blue shift of both the absorption and fluorescence spectra and also produces an increase in fluorescence intensity. These conclusions appear promising for the synthesis of fullerene derivatives with potential applications in optical devices.

ACKNOWLEDGMENTS

Preliminary photophysical results for $C_{70}Ph_{10}$ and $C_{70}Ph_8$ were kindly provided by E. J. J. Groenen *et al.* The authors thank S. Leach for useful comments. Thanks are due to the Fonds National de la Recherche Scientifique (FNRS/FRFC, Belgium) and the EU HCM Network "Formation, Stability and Photophysics of Fullerenes" (Contract No. ERBCHRXCT-940614) for financial support. The work in Mons is partly supported by the Belgian Federal Government "Pôle d'Attraction Interuniversitaire en Chimie Supramoléculaire et Catalyse Supramoléculaire (PAI 4/11)" and FNRS/FRFC. P.R.B. acknowledges the EPSRC for the award of an Advanced Fellowship.

¹Y.-P. Sun, in *Organic Photochemistry*, edited by V. Ramamurthy and K. S. Schanze (Marcel Dekker, New York, 1997), Vol. 1, p. 325.

²L. W. Tutt and A. Kost, *Nature* (London) **356**, 225 (1992).

³J. W. Arbogast, A. P. Darmanyan, C. S. Foote, M. M. Alvarez, S. J. Anz, and R. L. Whetten, *J. Phys. Chem.* **95**, 11 (1991).

⁴J. W. Arbogast and C. S. Foote, *J. Am. Chem. Soc.* **113**, 8886 (1991).

⁵J. L. Anderson, Y.-Z. An, Y. Rubin, and C. S. Foote, *J. Am. Chem. Soc.* **116**, 9763 (1994).

⁶P. S. Baran, R. R. Monaco, A. U. Khan, D. I. Schuster, and S. R. Wilson, *J. Am. Chem. Soc.* **119**, 8363 (1997).

⁷R. V. Bensasson, E. Bienvenue, J.-M. Janot, S. Leach, P. Seta, D. I. Schuster, S. R. Wilson, and H. Zhao, *Chem. Phys. Lett.* **245**, 566 (1995).

⁸D. M. Guldi, H. Hungerbühler, and K.-D. Asmus, *J. Phys. Chem.* **99**, 9380 (1995).

⁹S.-K. Lin, L.-L. Shiu, K.-M. Chien, T.-Y. Luh, and T.-I. Lin, *J. Phys. Chem.* **99**, 105 (1995).

¹⁰C. Luo, M. Fujitsuka, A. Watanabe, O. Ito, L. Gan, Y. Huang, and C.-H. Huang, *J. Chem. Soc., Faraday Trans.* **94**, 527 (1998).

¹¹B. Ma, C. E. Bunker, R. Guduru, X.-F. Zhang, and Y.-P. Sun, *J. Phys. Chem.* **101**, 5626 (1997).

¹²M. Maggini, G. Scorrano, M. Prato, G. Brusatin, A. Renier, R. Signorini, M. Meneghetti, and R. Bozio, *Adv. Mater.* **7**, 404 (1995).

¹³Y. Nakamura, T. Minowa, Y. Hayashida, S. Tobita, H. Shizuka, and J. Nishimura, *J. Chem. Soc., Faraday Trans.* **92**, 377 (1996).

¹⁴R. Signorini, M. Zerbetto, M. Meneghetti, R. Bozio, M. Maggini, C. De Faveri, M. Prato, and G. Scorrano, *Chem. Commun. (Cambridge)* **16**, 1891 (1996).

¹⁵Y.-P. Sun, G. E. Lawson, J. E. Riggs, B. Ma, N. Wang, and D. K. Moton, *J. Phys. Chem.* **102**, 5520 (1998).

¹⁶L. Udvardi, P. R. Surján, J. Kürti, and S. Pekker, *Synth. Met.* **70**, 1377 (1995).

¹⁷R. R. Williams, J. M. Zwier, and J. W. Verhoeven, *J. Am. Chem. Soc.* **117**, 4093 (1995).

¹⁸P.-F. Coheur, J. Cornil, D. dos Santos, P. R. Birkett, J. Liévin, J.-L. Brédas, J.-M. Janot, P. Seta, S. Leach, D. R. M. Walton, R. Taylor, H. W. Kroto, and R. Colin, *Synth. Met.* **103**, 2407 (1999).

¹⁹D. M. Guldi and K.-D. Asmus, *J. Phys. Chem.* **101**, 1472 (1997).

²⁰T. Hamano, K. Okuda, T. Mashino, K. Arakane, A. Ryu, S. Mashiko, and T. Nagano, *Chem. Commun. (Cambridge)* **1**, 21 (1997).

²¹H. Mohan, D. K. Palit, J. P. Mittal, L. Y. Chiang, K.-D. Asmus, and D. M. Guldi, *J. Chem. Soc., Faraday Trans.* **94**, 359 (1998).

²²D. K. Palit, H. Mohan, P. R. Birkett, and J. P. Mittal, *J. Phys. Chem.* **101**, 5418 (1997).

²³G. Schick, M. Levitus, L. Kvetko, B. A. Johnson, I. Lamparth, R. Lunkwitz, B. Ma, S. I. Khan, M. A. Garcia-Garibay, and Y. Rubin, *J. Am. Chem. Soc.* **121**, 3246 (1999).

²⁴K. Hutchison, J. Gao, G. Schick, Y. Rubin, and F. Wudl, *J. Am. Chem. Soc.* **121**, 5611 (1999).

²⁵P.-F. Coheur, J. Cornil, D. A. dos Santos, P. R. Birkett, J. Liévin, J. L. Brédas, D. R. M. Walton, R. Taylor, H. W. Kroto, and R. Colin, *J. Chem. Phys.* (in press).

²⁶A. G. Avent, P. R. Birkett, A. D. Darwish, H. W. Kroto, R. Taylor, and D. R. M. Walton, *Tetrahedron* **52**, 5235 (1996).

²⁷A. G. Avent, P. R. Birkett, M. Carano, H. W. Kroto, J. O. Lopez, F. Paolucci, S. Roffia, R. Taylor, N. Wachter, D. R. M. Walton, and F. Zerbetto (in preparation).

²⁸A. K. Rappé, C. J. Casewit, K. S. Colwell, W. A. Goddard III, and W. M. Skiff, *J. Am. Chem. Soc.* **114**, 10024 (1992).

²⁹M. J. S. Dewar, E. G. Zoebisch, E. F. Healy, and J. J. P. Stewart, *J. Am. Chem. Soc.* **107**, 3902 (1985).

³⁰M. J. Frisch, G. W. Trucks, H. B. Schlegel, P. M. W. Gill, B. G. Johnson, M. A. Robb, J. R. Cheeseman, T. Keith, G. A. Petersson, J. A. Montgomery, K. Raghavachari, M. A. Al-Laham, V. G. Zakrzewski, J. V. Ortiz, J. B. Foresman, J. Cioslowski, B. B. Stefanov, A. Nanayakkara, M. Challacombe, C. Y. Peng, P. Y. Ayala, W. Chen, M. W. Wong, J. L. Andres, E. S. Replogle, R. Gomperts, R. L. Martin, D. J. Fox, J. S. Binkley, D. J.

- Defrees, J. Baker, J. P. Stewart, M. Head-Gordon, C. Gonzalez, and J. A. Pople, GAUSSIAN 94, revision E. 1 (Gaussian Inc., Pittsburgh, PA, 1995).
- ³¹R. S. Mulliken, *J. Chem. Phys.* **33**, 1833 (1955).
- ³²T. Koopmans, *Physica (Utrecht)* **1**, 104 (1933).
- ³³Insight II User Guide, Molecular Simulations Inc., 1996.
- ³⁴R. J. Bell, P. Dean, and D. C. Hibbins-Buttler, *J. Phys. C* **3**, 2111 (1970).
- ³⁵D. A. dos Santos, C. Quattrochi, R. H. Friend, and J. L. Brédas, *J. Chem. Phys.* **100**, 3301 (1994).
- ³⁶M. C. Zerner, G. H. Loew, R. F. Kichner, and V. T. Mueller-Westerhoff, *J. Am. Chem. Soc.* **102**, 589 (1980).
- ³⁷N. Mataga and K. Nishimoto, *Z. Phys. Chem., Neue Folge* **13**, 140 (1957).
- ³⁸R. D. Bendale, J. D. Baker, and M. C. Zerner, *Int. J. Quantum Chem., Symp.* **25**, 557 (1991).
- ³⁹M. C. Zerner, in *Reviews in Computational Chemistry*, edited by K. B. Lipkowitz and D. B. Boyd (VCH, New York, 1995), Vol. 2, p. 313.
- ⁴⁰E. W. Godly and R. Taylor, *Pure Appl. Chem.* **69**, 1412 (1997).
- ⁴¹E. E. J. Groenen (private communication).
- ⁴²J. N. Murrell, *The Theory of the Electronic Spectra of Organic Molecules* (Spottiswoode, Ballantyne & Co. Ltd, London, 1963).